

A Numerical Study of Currents in the Taiwan Strait During Winter

Sen Jan¹, Ching-Sheng Chern² and Joe Wang²

(Manuscript received 2 September 1997, in final form 12 June 1998)

ABSTRACT

Hydrographic data acquired in the Taiwan Strait during the past decade suggest that, in winter, a zonal oceanic front develops over the Chang-yuen Ridge implying that the northward moving Kuroshio branch current cannot persistently hug the west coast of Taiwan as it flows toward the East China Sea as previous suggested. A three dimensional numerical model is used to study the dynamic process leading to the hydrographic pattern observed in the Taiwan Strait in winter. Model results show that the warm Kuroshio branch water in the Peng-hu Channel is blocked and then is forced to deflect westward as it impinges on the southern flank of the ridge. On the other hand, the monsoon-driven southward flowing cold China coastal water spreads southeastward into the northern Taiwan Strait when it passes around the Hai-tan Island. The cold water bulge occupies the upper layer of the area north of the ridge in time as winter progresses. The overall flow behavior in the strait in winter favors the formation of the oceanic front over the ridge between the two water masses.

(Key words: Taiwan Strait, Oceanic front, Numerical model)

1. INTRODUCTION

Taiwan Strait (TS) is a shallow water channel connecting the East China Sea (ECS) and the South China Sea (SCS). Figure 1 shows isobaths of the seas in and surrounding the TS. A distinct topographic feature in the TS is a ridge, Chang-yuen Ridge (CYR), extending westward from the middle of the west coast of Taiwan, to separate the strait into two basins. Early hydrographic investigation results suggested that there is a persistent northward current in the eastern TS carrying warm and saline water to the ECS (Chu, 1961; Wu, 1984; Chuang, 1985; etc.). Direct current measurements also indicate that, in winter, the mean current is northward in the Peng-hu Channel (PHC) and at the location marked CBK in Figure1 (Chuang, 1985; Wang *et al.*, 1988). According to results of hydrographic observations in the northern SCS and the ECS, Guan(1986) further speculated that this northward current in the TS connects the so called "South China Sea Warm Current" in the SCS and the "Taiwan Warm Current" in the

¹Tainan Hydraulics Laboratory, National Cheng Kung University, Tainan, Taiwan, ROC

²Institute of Oceanography, National Taiwan University, Taipei, Taiwan, ROC

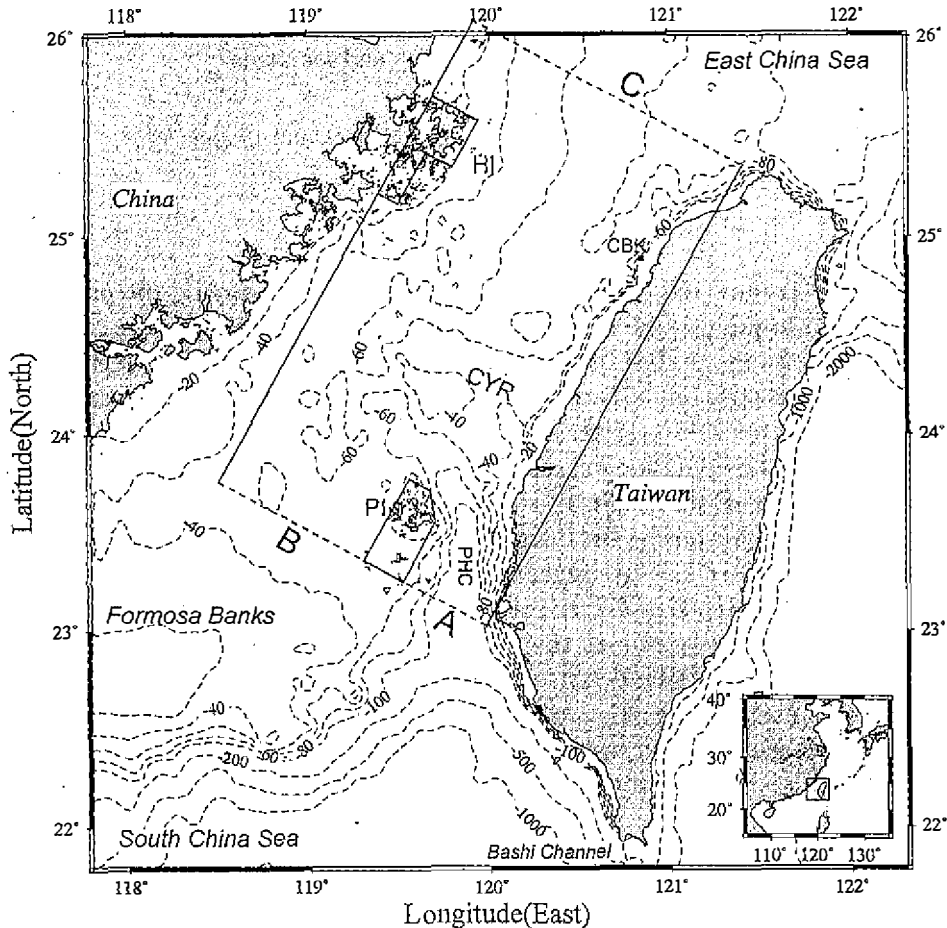


Fig. 1. Isobaths (in meters) in the Taiwan Strait and its adjacent seas. PHC is the Peng-hu Channel, PI is the Peng-hu Islands, CYR is the Chang-yuen Ridge and HI is the Hai-tan Island. The rectangle represents the model domain where dashed lines A, B and C are open boundaries across the southern entrance of the PHC, the Formosa Banks and the northern TS respectively.

ECS even in the winter NE monsoon season.

However, results from the hydrographic surveys in the TS during the past decade are not consistent with the above-mentioned conjecture. Fan and Yu (1981) found that, in winter, the northward warm and saline water, originally from the Kuroshio branch current, is blocked at the northern end of the PHC. The current measured at CBK by long term moored instruments, from October to January, shows that the mean current is northward. The temperature of this current is decreased from about 24°C to 19°C, and the salinity is reduced from 33.5psu to about 32.5~32psu (Wang *et al.*, 1988). The decrease of temperature and salinity at CBK in

winter implies that the cold and brackish coastal water from the China side may expand offshore to the northwest of Taiwan. These inferences are supported by results of conductivity-temperature-depth (CTD) surveys and satellite images of sea surface temperature (SST) in the TS during winter (Wang and Chern, 1988; 1989; 1993).

Figure 2 shows temperature and salinity distributions in the eastern TS during Nov. 12-16, 1988. The isotherms and isohalines at 10m depth, Figures 2(a) and 2(b), show that there is a zonal oceanic front over CYR, which is the most remarkable hydrographic pattern in the TS in winter (Wang and Chern, 1988). In the northern TS, water with low temperature ($<22^{\circ}\text{C}$) and low salinity ($<33\text{psu}$), the China coastal water, intrudes toward the southeast and reaches north of the CYR after about two months of the onset of the NE monsoon. Hydrographic data acquired in the western TS in winter, on the other hand, suggest that this cold coastal water can be driven southward to the north edge of the Formosa Banks (Xiao and Cai, 1988). In the PHC, water with high temperature ($>24^{\circ}\text{C}$) and high salinity ($>34\text{psu}$), the Kuroshio branch water, is confined south of the CYR. This warm water may deflect into the area west of the Peng-hu Islands where the salinity will increase in time from late autumn to early spring (Wang and Chern, 1993). Figures 2(c) and 2(d) respectively show the temperature and salinity distributions at a zonal transect, line AB in Figure 2. The isotherms and isohalines shown in Figures 2(c) and 2(d) indicate that the cold water bulge occupies the upper layer of the northeastern TS. The figures also imply that the salinity rather than the temperature structure maintains the stratification of the water column in the northern TS in winter. Figures 2(e) and 2(f) respectively show the temperature and salinity distributions at a meridional transect across the front, line CD in Figure 2. Figures 2(e) and 2(f) show that the front is weakly stratified in vertical, and the horizontal gradients of temperature and salinity across the front are about $2^{\circ}\text{C}/30\text{km}$ and $1\text{psu}/30\text{km}$.

The hydrography in the TS in winter has been well documented, as mentioned above, but there still is a lack of in-depth studies about the dynamic process leading to the observed hydrography. That motivates us to study the formation of the front and the influence of the through-flow and the topography on the flow field by using a numerical model. The flow field related to the observed wintertime hydrography is generated at first. Then, four main ingredients, the forcing of surface wind stress, the cooling of the sea surface water by the atmosphere, the steering of the bottom topography and the influence of the through-flow transport are employed to examine the overall circulation pattern in winter. The modeled flow fields are compared with the observed hydrography. The influences of the ingredients on the hydrographic pattern are discussed.

2. MODEL FORMULATION

The model developed by Semtner (1974, 1986) solves the three-dimensional momentum, continuity, temperature and salinity equations with Boussinesq, hydrostatic and rigid-lid approximations. The density is calculated from the equation of state as modified by Mellor (1991). The model domain, as shown by the rectangle in Figure 1, has 40 and 65 grids in the x and y directions, respectively, with a grid size of 5km, and 10 layers in the vertical with a layer thickness of 10m. The lower left corner of this domain is set at $23^{\circ} 55' \text{N}$ and $118^{\circ} 25' \text{E}$. Figure 3 shows the model basin, which is close to the bottom topography in the TS as shown in Figure

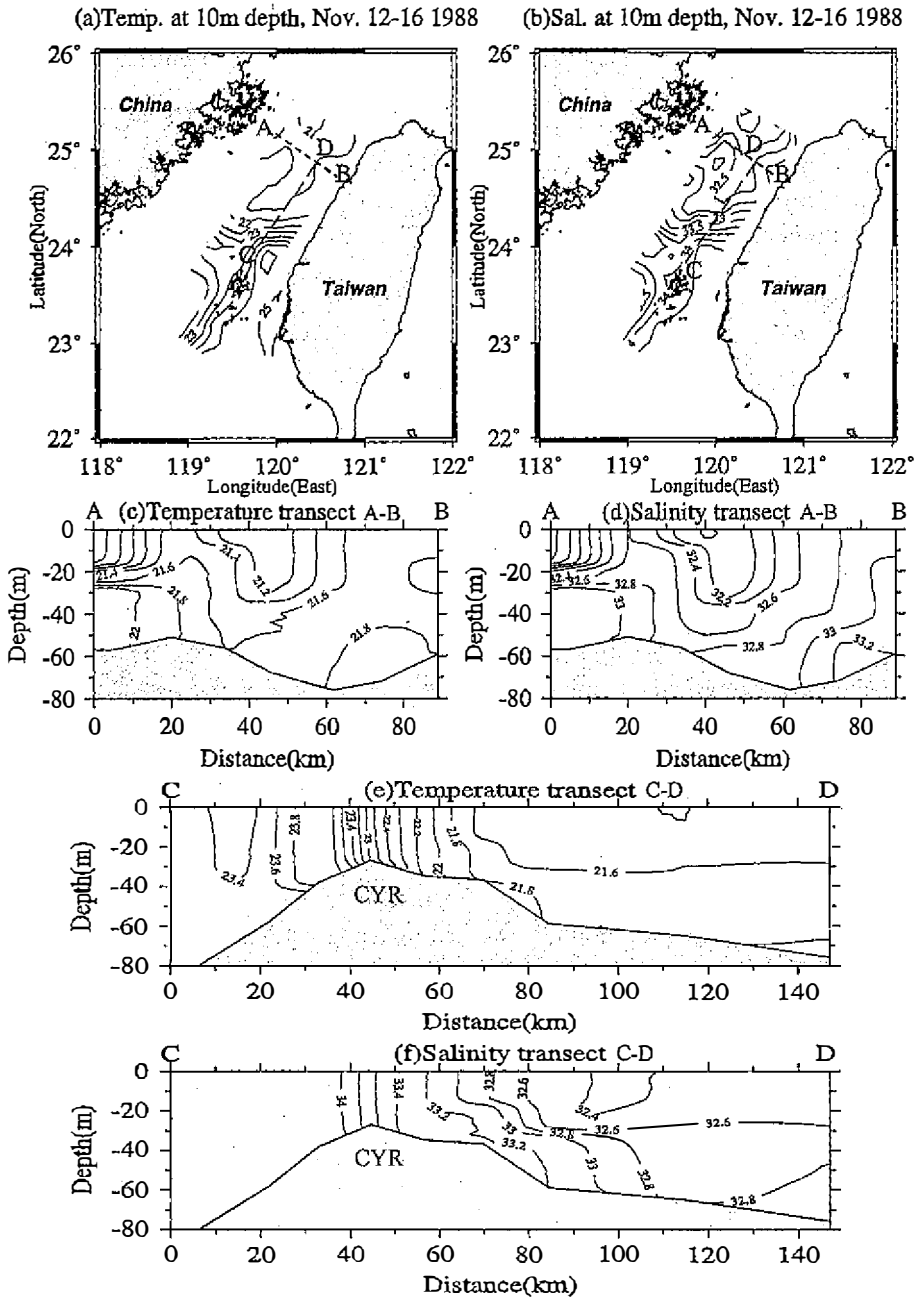


Fig. 2. Temperature(°C) and salinity(psu) distributions in the Taiwan Strait during Nov. 12-16, 1988. (a) and (b) at 10m depth; (c) and (d) at a zonal transect along dashed line A-B; (e) and (f) at a meridional transect along dashed line C-D.

1. Variables, such as temperature, salinity, density and transport stream-function, are calculated at the center of each grid box. The through-flow transports across open boundaries A, B and C, dashed lines in Figure 1, account for flows through the PHC, across Formosa Banks and across the northern TS respectively. A quadratic stress law and no flux conditions for temperature and salinity are applied at the bottom. At the rigid surface, the salt flux is zero, while the heat flux is not zero. The wind stresses at the rigid surface are applied as

$$\rho_0 \nu \frac{\partial(u,v)}{\partial z} = (\tau_x, \tau_y),$$

where ρ_0 is the reference density, ν is the vertical eddy viscosity, u and v are the velocity components in the x and y directions, z is the vertical coordinate, and τ_x and τ_y are the sea

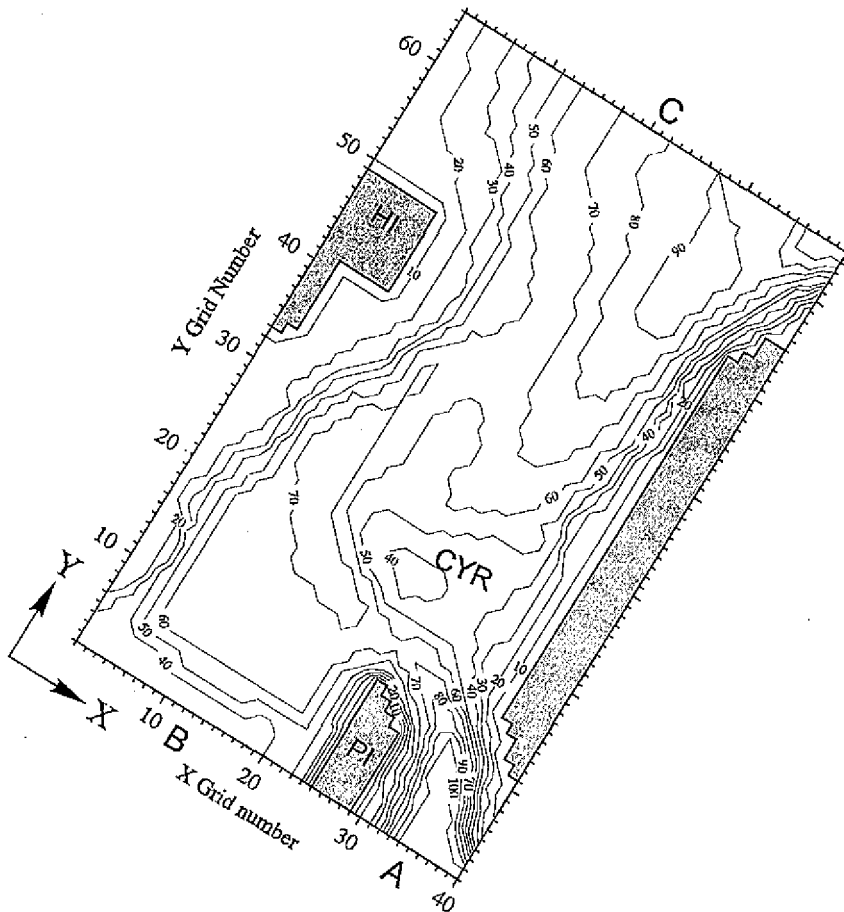


Fig. 3. Isobaths (in meters) in the model basin.

surface wind stresses in the x and y directions.

In order to generate the onset of the winter currents, the summertime flow field is spun up from rest and used as the initial condition. At the open boundary, the vertical transects of the temperature and salinity, as in Figure 5 of Wang and Chern (1992), are initially fixed. The normal gradient conditions for temperature and salinity are used at open boundaries B and C. The model ocean is driven with volume transports of 1 Sv ($10^6 \text{ m}^3/\text{s}$) inflow from A, zero at B and 1 Sv outflow through C. The horizontal and vertical mixing coefficients respectively are $2.5 \times 10^6 \text{ cm}^2/\text{s}$ and $5 \text{ cm}^2/\text{s}$ for the momentum, temperature and salinity balance equations. The non-dimensional bottom drag coefficient is 0.005.

After about 120 days of numerical integration, the flow field approaches a quasi-steady state. Thereafter, the flow field has no appreciable changes. The solution at day 200 is chosen to be the initial condition. Figure 4 shows the initial flow fields at 15m(surface layer) and 45m(bottom layer) depths. Briefly, the warmer surface water coming from the PHC crosses over the CYR and then flows along the west coast of Taiwan to reach the northeastern TS. The cold bottom water from the PHC is blocked south of the ridge and then turns northwestward toward the western TS. The dynamic process of this summertime circulation has been discussed in the study of Jan *et al.* (1994).

To simulate winter currents, a northerly mean wind stress of $1.2 \text{ dyne}/\text{cm}^2$ is applied at the sea surface except for within five grid intervals next to each of the open boundaries where the wind stress is set to zero to avoid generating noise. At the rigid sea surface, the salt flux remains zero, while heat loses to the atmosphere at a rate of $240 \text{ Watts}/\text{m}^2$ (Ishii and Kondo, 1987). At the open boundary A, the northward volume transport is decreased with time from 1 Sv to 0.2 Sv; the vertical profiles of the temperature and salinity are linearly changed to the observed data shown in Figure 5. At the open boundary B, the transport is increased with time from zero to 0.4 Sv out of the domain; the temperature and salinity gradients in the y direction are set to zero. At the northern open boundary C, in order to keep volume conservation in the model, a volume transport of 0.2 Sv southward into the model is implemented; the vertical structures of the temperature and salinity for inflows are given as the profiles shown in Figure 6, and zero normal gradient conditions for the two variables are used for outflows. All these variable changes are implemented linearly with time during the first 30 days of integration, and then held fixed for 30 more days of integration. The horizontal and vertical mixing coefficients are the same as those used for the generation of the initial field. The model result is regarded as case W0.

3. MODEL RESULTS

Figure 7 shows the velocity vectors, isotherms and isohalines at 15m and 45m depths of case W0 at day 60. At the surface layer, the China coastal water, moves southward along the China coast and crosses through the open boundary B out of the model. The mean velocity of this longshore current can reach a speed as large as $20 \text{ cm}/\text{s}$. A part of this cold water protrudes southeastward off east of the Hai-tan Island, and turns counterclockwise north of the CYR toward the northeastern bank of the TS. It carries low temperature ($<21^\circ\text{C}$) and low salinity ($<33\text{psu}$) water to offshore area northwest of Taiwan with a northward velocity of about $10 \text{ cm}/\text{s}$. As a result, the temperature and salinity decrease there in time as shown in Figure 8, time

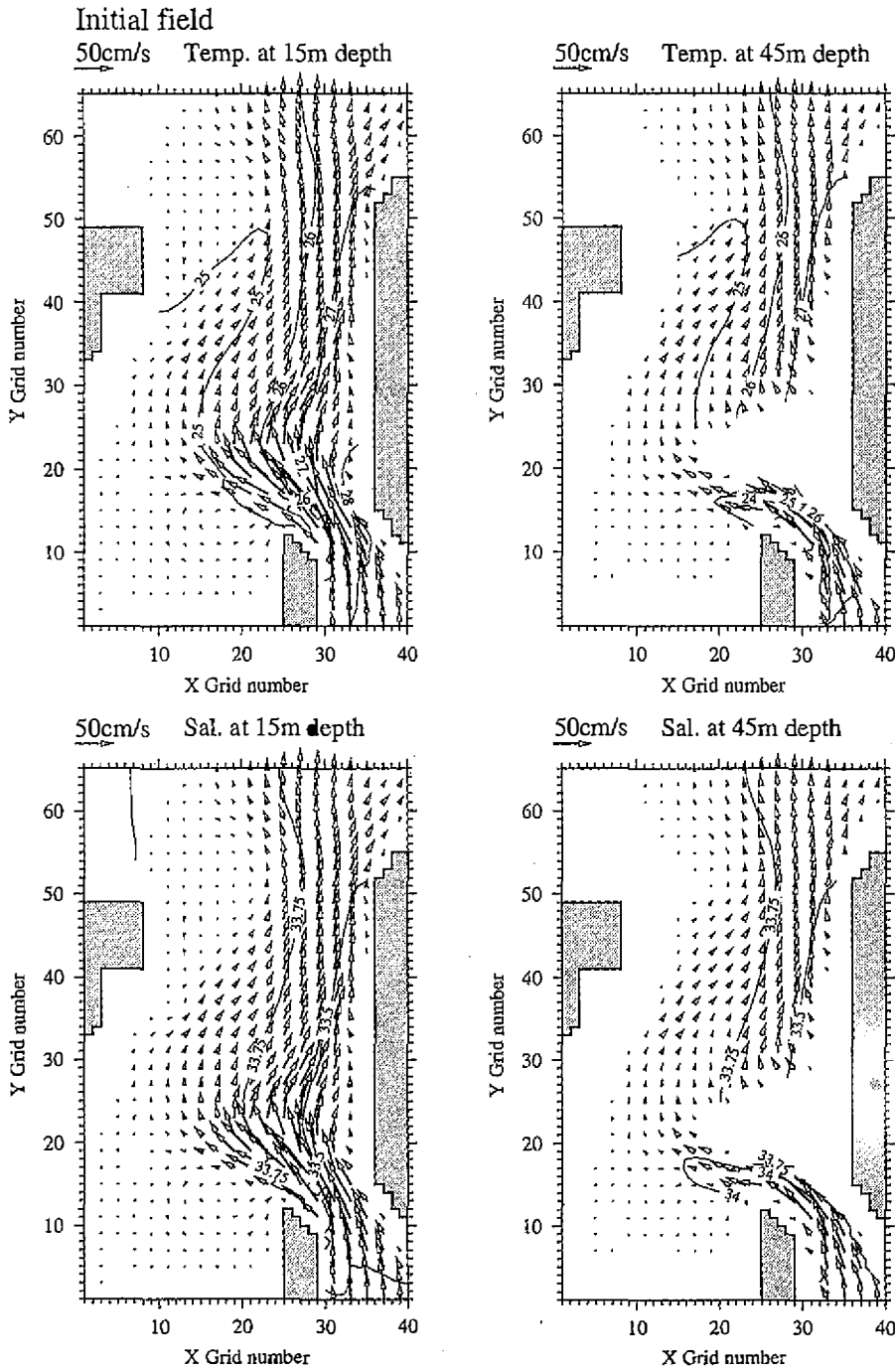


Fig. 4. Horizontal velocity vectors, isotherms(upper panels) and isohalines(lower panels) at 15m and 45m depth of the initial flow field at day 200.

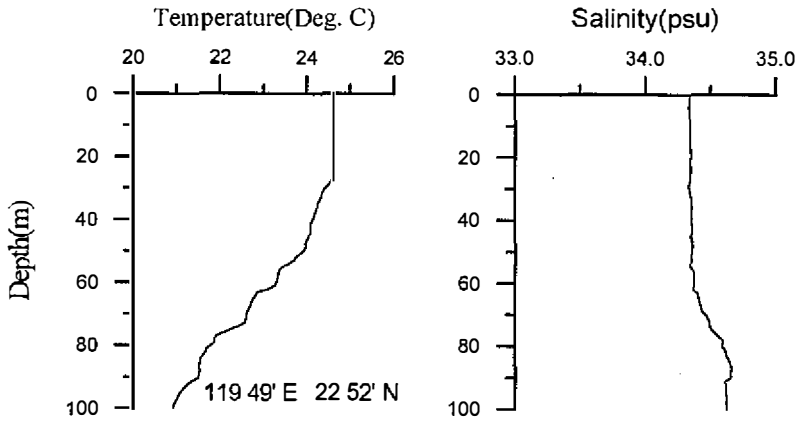


Fig. 5. Temperature and salinity profiles at the southern entrance of the PHC on Nov. 12, 1988. The CTD station located at $22^{\circ} 50' N$ and $119^{\circ} 49' E$.

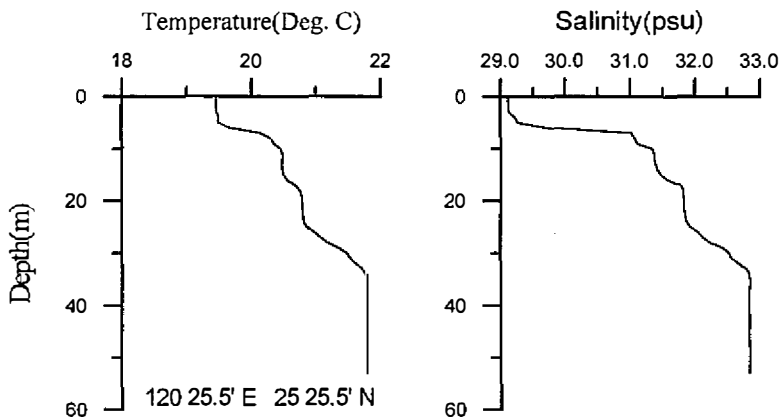


Fig. 6. Temperature and salinity profiles in the northern TS on Nov. 15, 1988. The CTD station located at $25^{\circ} 25.5' N$ and $120^{\circ} 21' E$.

series of the two variables at grid numbers $X=32$ and $Y=25$ at 25m depth during the integration period. Figure 9 shows temperature and salinity distributions at the zonal transect $Y=50$ across the northern TS of case W0. It illustrates that the cold water from China side extends toward the upper layer of the eastern portion. Therefore the warmer and more saline water is confined over the bottom near the eastern boundary. The resemblance of the vertical structure of temperature and salinity between the model result, Figure 9, and the observation result, Figure 2(c) and 2(d), is clear at least in the eastern TS.

At southeast part of the flow field, Figure 7, the Kuroshio branch water enters into the PHC through the open boundary A. As this warm water impinges on the CYR, a part of it

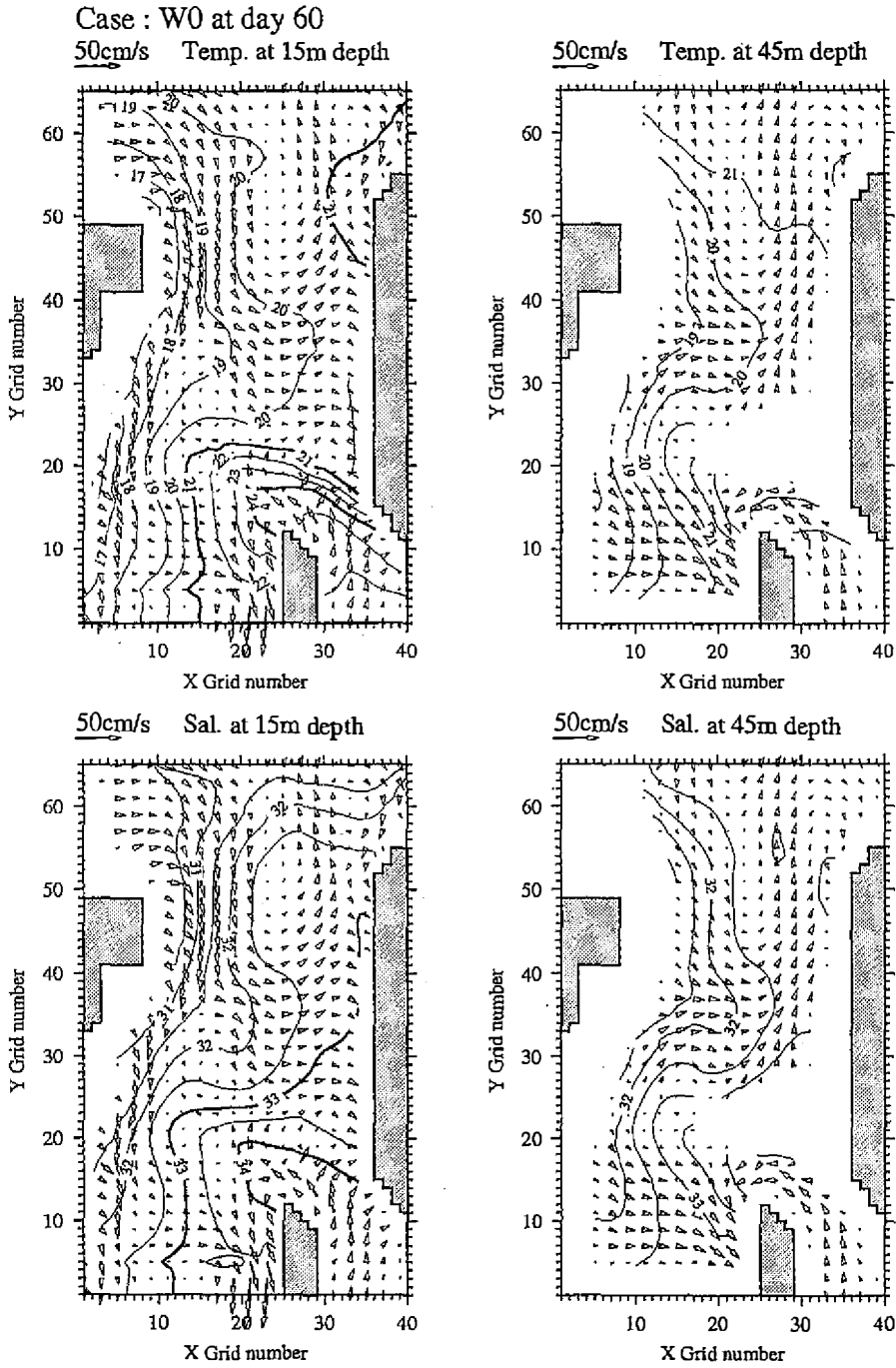


Fig. 7. Horizontal velocity vectors, isotherms(upper panels) and isohalines(lower panels) at 15m and 45m depths of case W0 at day 60.

deflects westward; the remainder turns eastward and forms a weak clockwise eddy over the CYR. The flow behavior of the China coastal water and the Kuroshio branch water favors the frontogenesis. As expected, a zonal oceanic front develops between the two water masses over the CYR. Figure 10 shows temperature and salinity transects at the meridional section $X=25$ across the front. The horizontal differences of temperature and salinity across the front, between grid numbers $Y=19$ and $Y=26$, are about 2.5°C and 1 psu respectively, which are nearly the same magnitudes as those shown in Figure 2(e) and Figure 2(f).

The flow field at 45m depth in Figure 7 indicates that the bottom circulation has the same pattern as that at the surface layer. It is worth noting that a part of the bottom water coming from the PHC can flow around the CYR into the northern TS, and mixes with the surface water there. The horizontal difference of the density between the northern and the southern TS is gradually reduced due to the bottom intrusion and the vertical mixing processes.

Figure 11 shows the magnitude of all terms in the x and y components of the momentum equation at 15m depth along the meridional section $X=33$ for the current of case W0. The x component of the momentum equation is in geostrophic balance in PHC between grid numbers $Y=1$ and $Y=12$, Figure 11(a). While the nonlinear terms are important in the y component of the momentum equation near the steep rise of the bottom topography at grid number $Y=10$, Figure 11(b). The Rossby number, U/fL , of the current in the PHC is estimated of about 0.13 with the velocity $U=20$ cm/s, the Coriolis parameter $f=5.92 \times 10^{-5} \text{ s}^{-1}$ and the width of the PHC $L=25$ km. Hence the northward current from the PHC will follow local isobaths on the southern side of the CYR due to its low Rossby number and weak stratification.

The modeled flow field of case W0 is in a good agreement with the observed hydrography, Figure 2, and may be regarded as the typical circulation regime in the Taiwan Strait during the winter season.

4. DISCUSSION AND CONCLUDING REMARKS

The wind stress of the NE monsoon is the main forcing driving the China coastal water moving southward into the TS. The cooling of the sea surface water may strengthen this southward moving longshore current due to the thermal wind relation, and may enhance the temperature contrast across the front. In addition to the wind stress and the heat loss from the sea surface, the through-flow and the complicated bottom topography are also important to the wintertime circulation in the TS. In case W0, the volume transport across the width of the northern TS is 0.2 Sv southward which is consistent with that estimated by Wyrтки (1961). However, Fang *et al.* (1989) estimated that the volume transports across the Formosa Banks and the PHC respectively are 0.6 Sv and 0.4 Sv northward in winter. This yields a transport of 1 Sv northward across the width of the strait, which is contrary to that in our model. A contrast numerical experiment, case W1, is designed to identify the reasonable transport magnitude and direction of the through-flow in the TS in winter.

Moreover, the role of the CYR on the formation of the zonal front has yet to be examined. A flow field over the bottom topography without the CYR, case W2, is generated and then is compared with that of case W0. Table 1 lists the transports of the through-flow across open boundaries A, B and C and the bottom topography used for the two experiments. In case W1, volume transports at the open boundaries are linearly adjusted from those set in the initial flow

field to the values listed in Table 1 during the first 30 days of integration. The boundary conditions and the mixing coefficients for the two cases are the same as those used in case W0. Each of the experiments is integrated for 60 days. The model results are as follows.

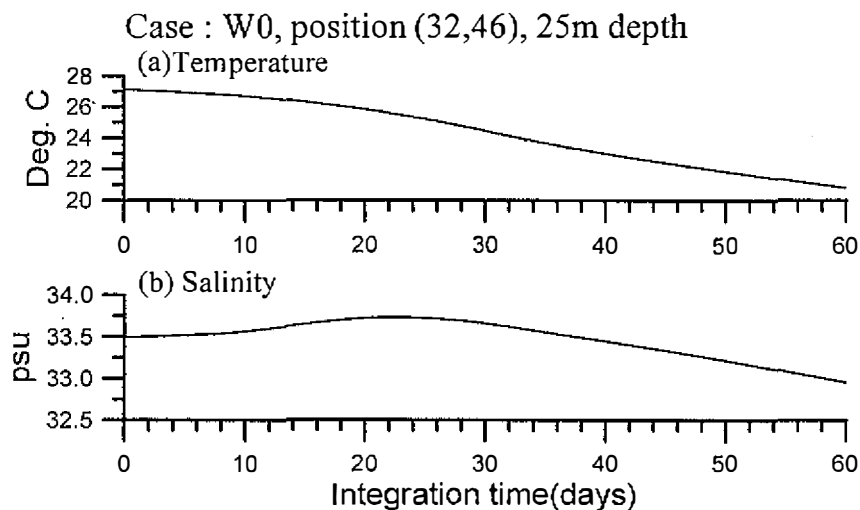


Fig. 8. Time series of temperature and salinity at grid numbers X=32 and Y=46 at 25m depth of case W0 during the integration period.

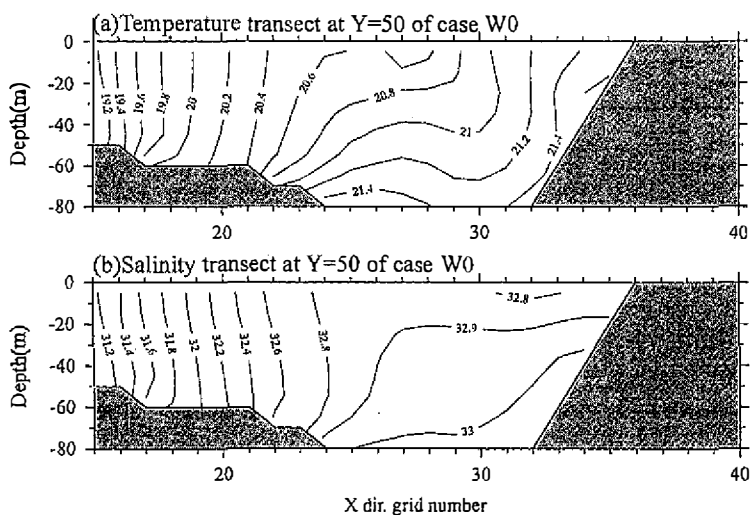


Fig. 9. Temperature(a) and salinity(b) distributions at the zonal transect along grid number Y=50 from X=15 to X=40 of case W0.

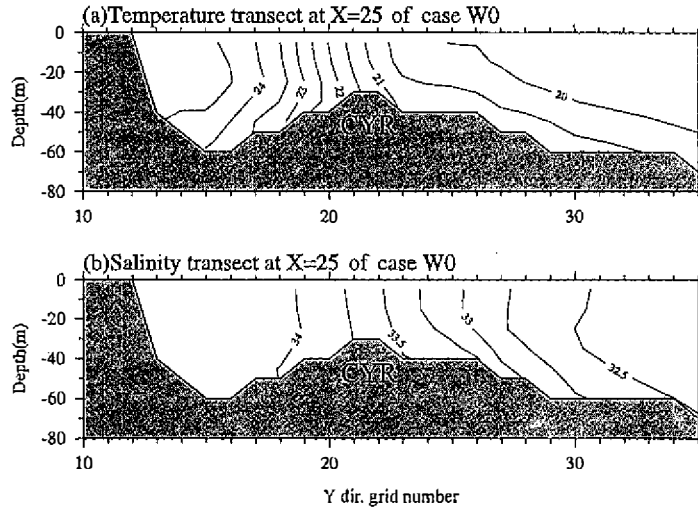


Fig. 10. Temperature(a) and salinity(b) distributions at the meridional transect along grid number $X=25$ from $Y=10$ to $Y=35$ of case W0.

Table 1. Volume transports ($\times 10^6 \text{m}^3/\text{s}$) of the through-flow across open boundaries A, B and C and the bottom topography used for cases W1 and W2. Positive and negative transport values mean inflow and outflow respectively.

Case	A	B	C	Topography condition
W1	0.4	0.6	1	same as W0
W2	0.2	-0.4	-0.2	without CYR

4.1 Case W1

Figure 12 shows flow fields at 15m and 45m depths of case W1 at day 60. The circulation pattern differs from that of case W0 in obvious ways. In case W1, the cold and brackish water from China side is nearly confined east of Hai-tan Island. The warm and saline water coming across open boundaries A and B moves over and around the CYR and then turns toward the northwest coast of Taiwan. This high temperature ($>24^\circ\text{C}$) and high salinity ($>34\text{psu}$) water tongue protrudes northward along the west coast of Taiwan with a velocity up to about 50 cm/s which is much stronger than the mean velocity, $10\text{--}15 \text{ cm/s}$, measured by Wang *et al.* (1988) at CBK in winter. Figure 13 shows time series of temperature and salinity at grid numbers $X=32$ and $Y=46$ at 25m depth during the integration period. The increase of salinity at this site is contrary to the model result of case W0, Figure 8, and the result of the field observation at CBK. The flow fields also show that a frontal structure develops north of the ridge CYR along 60m isobath.

Case : W0

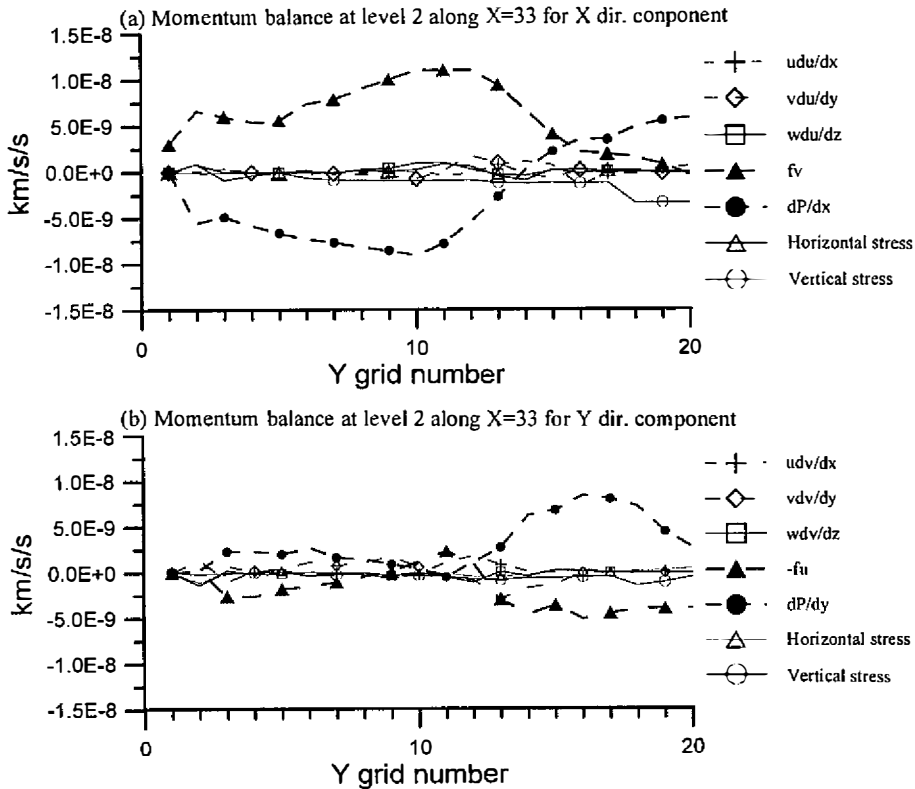


Fig.11. Magnitude of terms in the x -component (a) and y -component (b) of the momentum equation at 15m depth along the meridional section $X=33$ of the flow field shown in Figure 7. (u,v,w) are the velocity components in the (x,y,z) directions, f is the Coriolis parameter and P is p/ρ where p is the pressure and ρ is the reference water density.

The through-flow transport of 0.4 Sv northward through PHC was calculated from the current data acquired by Chuang (1986) in PHC in early spring from March to April. The mean velocity during this period is greater than that in winter. Therefore the flow transport through the PHC in case W1 may be over-estimated and can not be regarded as the winter condition. On the other hand, the transport of 0.6 Sv across the Formosa Banks was calculated by utilizing the current data continuously measured for 25 hours. The current shipboard measurement was usually done during the short period when winter monsoon weakened. In winter, the sea surface elevation in the southern TS can be piled up by the wind stress of the NE monsoon. As the NE monsoon intermittently weakened or ceased for 1 to 2 days, the sea surface elevation can not be maintained and a northward transient flow will be induced by the pressure gradient force related to the sea surface level difference between the northern and the

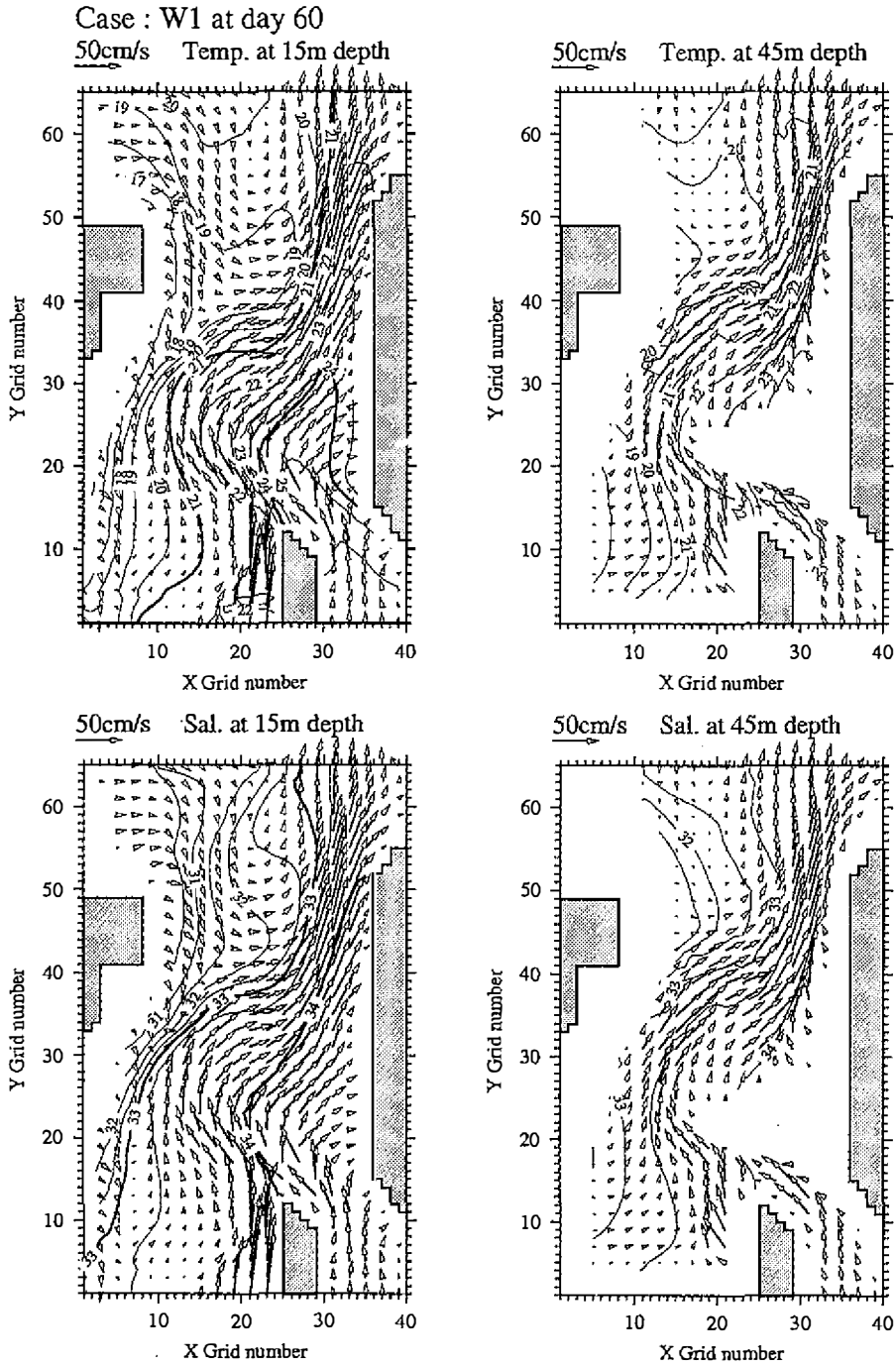


Fig. 12. Horizontal velocity vectors, isotherms(upper panels) and isohalines(lower panels) at 15m and 45m depths of case W1 at day 60.

southern TS. Hence the through-flow transport across the Formosa Banks estimated by Fang *et al.* (1989) may be a transient rather than the mean condition in winter.

The flow behavior of case W1 can not lead to the hydrography observed in winter, Figure 2. This implies that the through-flow volume transports used in case W0 are more reasonable than those used in case W1. Although the flow field of case W1 is not a usual winter regime in the TS, it is related to the hydrographic feature in the spring season, which can be identified by results of the CTD surveys and images of the SST. This will be discussed in our future study.

4.2 Case W2

The model conditions for Case W2 is the same as those for case W0 except that the CYR is removed from the model basin. Figure 14 shows flow fields of case W2 at 15m and 45m depths at day 60. The water column with high temperature ($>22^{\circ}\text{C}$) and high salinity ($>33.5\text{psu}$) moving from the PHC extends toward west and north and forms a wedge-like shape with its thin end heading north and hugging the west coast of Taiwan. The northward warm water encounters the cold water from China side at the central part of the strait where develops a front aligned in the NE-SW directions. The alignment and the location of the front differ from those of case W0 in the eastern TS. Therefore the flow field of case W2 deviates from the typical hydrographic feature in the strait in winter.

Results from the comparison between flow fields of cases W0 and W2 indicate that the CYR has the effect on guiding the front aligned E-W in the eastern TS. As the northward flow in the PHC, open arrows in Figure 15, moves onto the steep rise topography near the northern end of the PHC, it is forced to turn west along isobaths both due to its low Rossby number and the retardation of the northeasterly wind stress. The warm Kuroshio branch water is therefore blocked south of the ridge. The cold China coastal water, dark arrows in Figure 15, spreads to the east from east of the Hai-tan Island due to the deflection of the shoreline. The wind stress

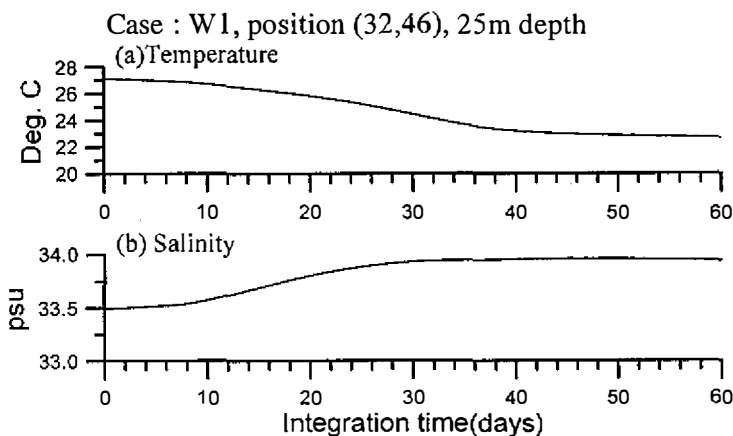


Fig. 13. Time series of temperature and salinity at grid numbers $X=32$ and $Y=46$ at 25m depth of case W1 during the integration period.

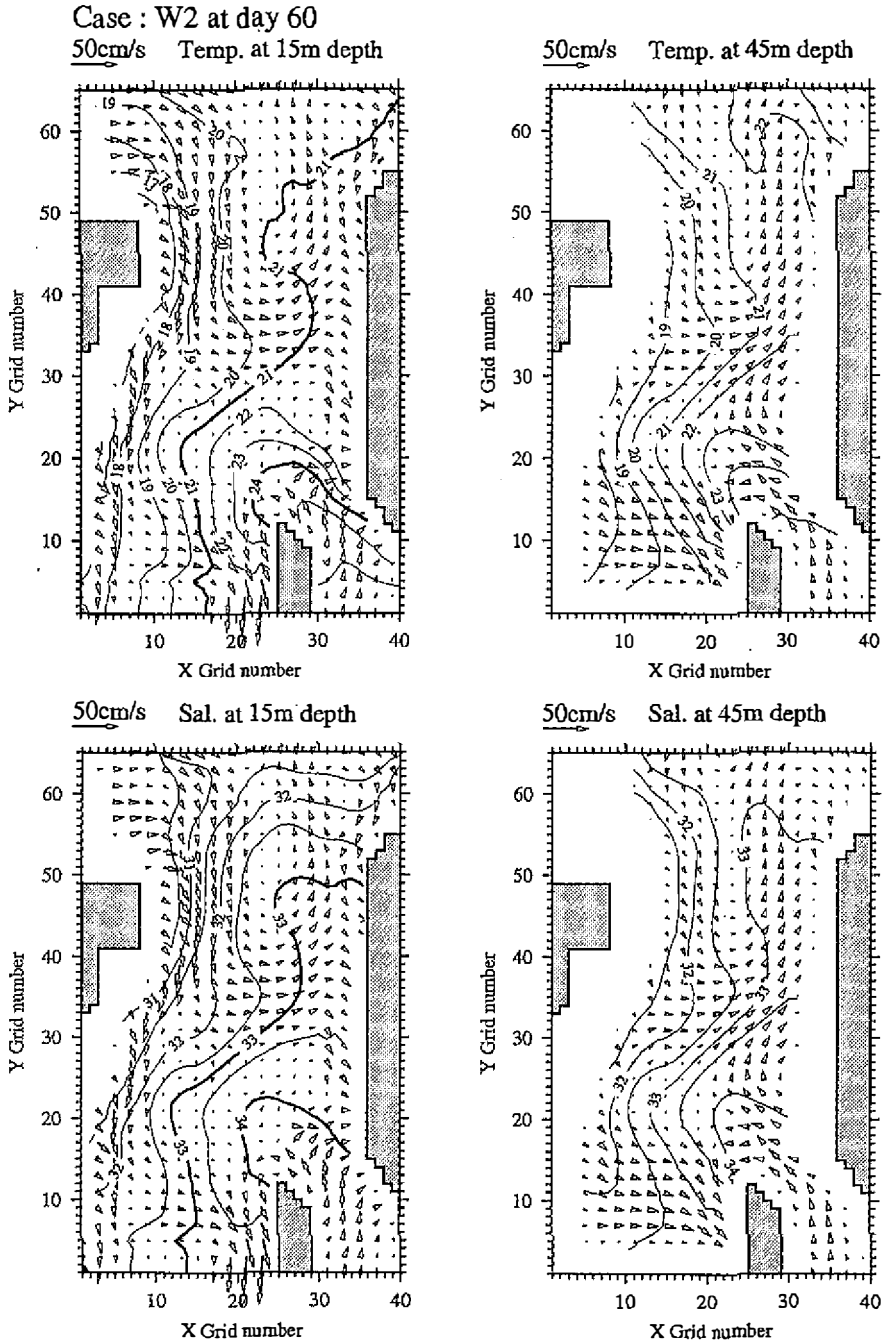


Fig. 14. Horizontal velocity vectors, isotherms(upper panels) and isohalines(lower panels) at 15m and 45m depths of case W2 at day 60.

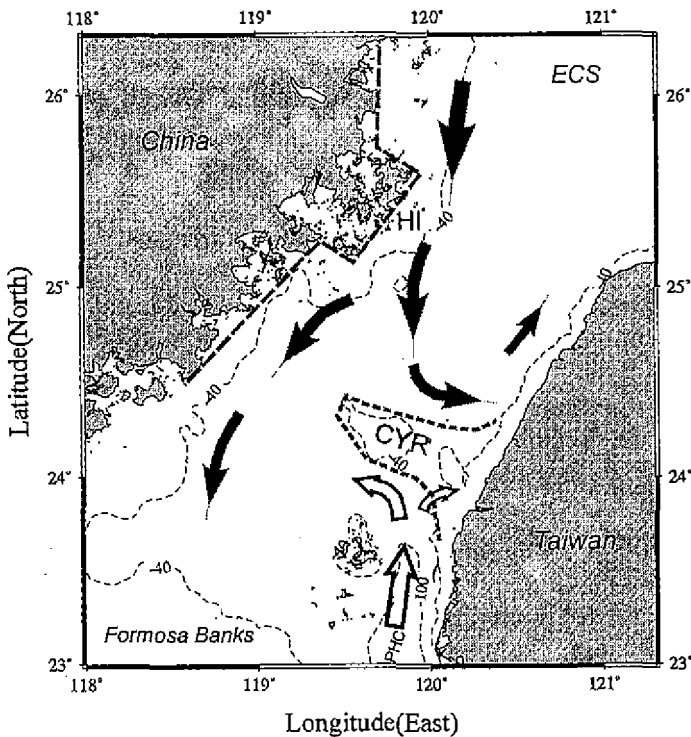


Fig. 15. A schematic showing the formation of the front over the CYR in the Taiwan Strait in winter. Dark and open arrows respectively represent the China coastal water and the Kuroshio branch water. The long dashed line illustrates that the deflection of the shoreline of China coast; the short dashed line represents the margin of the CYR.

may drive this cold water bulge further south to the north edge of the ridge. Over the CYR, a zonal front develops between the two water masses in time as winter progresses. Without the blocking of this ridge, the warm water may protrude northward along the west coast of Taiwan and the front will be pushed to the central part of the strait aligned NE-SW.

To summarize, the hydrographic survey results together with model results indicate that the warm Kuroshio branch water is blocked south of the CYR and thus can not persistently move northward along the west coast of Taiwan as previous inferred. The model results also suggest that the currents in the Taiwan Strait in winter are dominated by the transports of the through-flow, the CYR, the NE monsoon as well as the sea surface cooling effect. The modeled flow field of case W0 shows that the northward flowing Kuroshio branch water is blocked and then is forced to deflect westward as it impinges on the CYR. The monsoon-driven, moving southward China coastal water, on the other hand, spreads from east of the Hai-tan Island toward the southeastern TS and occupies the upper layer north of the CYR. This circulation pattern in the TS in winter favors the formation of the oceanic front over the ridge and leads the front aligned in E-W directions. The sea surface water cooling by the atmosphere further enhances the temperature difference across the front. The modeled flow field is consistent with results of the hydrographic observations.

Acknowledgements We deeply thank Professors Y. Hsueh and S.-Y. Chao for their useful comments and suggestions to improve the manuscript.

REFERENCES

- Chuang, W.-S., 1985: Dynamics of subtidal flow in the Taiwan Strait. *J. Oceanogr. Soc. Japan*, **41**, 65-72
- Chuang, W.-S., 1986: A note on the driving mechanisms of current in the Taiwan Strait. *J. Oceanogr. Soc. Japan*, **42**, 355-361
- Fan, K.-L., and C.-Y. Yu, 1981: A study of water masses in the seas of southernmost Taiwan. *Acta Oceanogr. Taiwanica*, **12**, 94-111
- Fang, G., B. Zhao, and Y. Zhu, 1989: Water transports through the Taiwan Strait and the East China Sea measured with current meters. in Programme and Abstracts, JECSS, 5th Workshop, Kangnung, Korea
- Guan, B., 1986, A sketch of the current structures and eddy characteristics in the East China Sea. *Studia Marina Sinica*, **27**, 1-20(in Chinese)
- Ishii, T., and J. Kondo, 1987: Seasonal variation of the heat balance of the East China Sea, *Tenki*, **34**, 517-526(in Japanese)
- Jan, S., C.-S. Chern, and J. Wang, 1994: A numerical study on currents in Taiwan Strait during summertime. *La mer*, **32**, 225-234
- Mellor, G. L., 1991: An equation of state for numerical models of oceans and estuaries. *J. Atmos. Oceanic Tech.*, **8**, 609-611
- Semtner, A. J., 1974: An oceanic general circulation model with bottom topography. Numerical simulation of weather and climate, Tech. Rep. **9**, Dept. of Meteorology, UCLA, 99pp
- Semtner, A. J., 1986: Finite difference formulation of a world ocean model. In: J. J. O'Brien, (Ed.), Proceedings of the NATO advanced study institute on advanced physical oceanographic numerical modelling, D. Reidel Publishing Co., Dordrecht, 608pp
- Wang, J. and C.-S. Chern, 1988: On the Kuroshio branch in the Taiwan Strait during wintertime. *Prog. Oceanogr.*, **21**, 469-491
- Wang, J., and C.-S. Chern, 1989: On cold water intrusions in the eastern Taiwan Strait during the cold season. *Acta Oceanogr. Taiwanica*, **22**, 43-67 (in Chinese)
- Wang, J., and C.-S. Chern, 1992: On the distribution of bottom cold waters in Taiwan Strait during summertime. *La mer*, **30**, 213-221
- Wang, J., C.-S. Chern, J.-S. Chern, and Y.-Y. Huang, 1988: Oceanographic observations at CBK-11 platform and the nearby area. Special publ. No. **57**, Institute of Oceanography, National Taiwan University, 279pp (in Chinese)
- Wang, J., C.-S. Chern, N.-K. Liang and M.-Y. Shyu, 1993: A preliminary study on the response of subtidal flows to the winter monsoon in the vicinity of Formosa Banks. *Acta Oceanogr. Taiwanica*, **31**, 1-43
- Wu, B., 1984: Some problems on circulation study in Taiwan Strait. Collected oceanic works, China ocean press, **7**, 24-35 (in Chinese)
- Wyrtki, K., 1961: Physical oceanography of the southeast Asia waters. Scientific results of marine investigations of the South China Sea and Gulf of Thailand. *NAGA Report*, **2**, 195pp
- Xiao, H., and S. Cai, 1988: Distribution characters of sea temperature and salinity in western Taiwan Strait. *J. Oceanogr. in Taiwan Strait*, **7**, 227-234 (in Chinese)